Cell

The Retromer Protein VPS29 Links Cell Polarity and Organ Initiation in Plants

Yvon Jaillais,[1] Martina Santambrogio,[1] Frédérique Rozier,[1] Isabelle Fobis-Loisy,[1] Christine Miège,[1] and Thierry Gaude[1,*]

[1]Reproduction et Développement des Plantes, Institut Fédératif de Recherche 128, Centre National de la Recherche Scientifique, Institut National de la Recherche Agronomique, Université Claude Bernard Lyon I, Ecole Normale Supérieure de Lyon, 46 allée d'Italie 69364 Lyon Cedex 07, France

*Correspondence: thierry.gaude@ens-lyon.fr

DOI 10.1016/j.cell.2007.08.040

SUMMARY

A key feature of plants (as opposed to animals) is their ability to establish new organs not only during embryogenesis, but also throughout their development. A master regulator of organ initiation in plants is the phytohormone auxin. Auxin acts locally as a morphogen and is directionally transported from cell to cell by polarized auxin efflux carriers, termed PIN-FORMED (PIN) proteins. Here we report that the *Arabidopsis* ortholog of the yeast and mammalian vacuolar protein sorting 29 (VPS29), a member of the retromer complex, mediates the formation of new axes of development. Furthermore, we show that VPS29 is required for endosome homeostasis, PIN protein cycling, and dynamic PIN1 repolarization during development. We propose a model that links VPS29 function, PIN1 polarity, and organ initiation in plants.

INTRODUCTION

Auxin is a phytohormone required for numerous aspects of plant development such as cell growth and division, pattern formation, organ emergence, phototropism and gravitropism, vascular tissue development, apical dominance, and phyllotaxy (Leyser, 2006). Auxin acts locally as a morphogen and is actively transported from its site of synthesis toward its site of action by plasma-membrane (PM)-localized auxin influx carriers (e.g., AUX or PGP4) or efflux carriers (e.g., PIN, PGP1, or PGP19) (Leyser, 2006). PIN proteins are polarly localized, and this polarity directly regulates the direction of auxin flux (Wisniewska et al., 2006). PIN proteins cycle continuously between the PM and endosomal compartments (Geldner et al., 2001, 2003; Jaillais et al., 2006). When this endocytic trafficking is chemically blocked by inhibitors, or genetically impaired, auxin transport is compromised (Geldner et al., 2001, 2004). The GDP/GTP Exchange Factor for ARF GTPases GNOM is required for embryo development and proper PIN1 polarity (Steinmann et al., 1999). Interestingly, GNOM is an endosomal protein required for PIN1 endocytic cycling (Geldner et al., 2003). Also, endocytosis seems to be directly modulated by auxin levels, being inhibited at some auxin concentrations and promoted at others (Abas et al., 2006; Paciorek et al., 2005). Finally, endocytosis is involved in downregulation of PIN2 during the gravitropic response (Abas et al., 2006).

We recently showed that the intracellular routes taken by PIN proteins during their endocytic trafficking are highly differentiated (Jaillais et al., 2006). PIN1 used a GNOM endosomal pathway for its trafficking, while PIN2 can use another endosomal compartment for its recycling or degradation, which is characterized by the presence of the SNX1 protein (Jaillais et al., 2006). SNX1 is the first described plant sorting nexin and is orthologous to the human SNX1 (Vanoosthuyse et al., 2003). *Hs*SNX1 is a member of the retromer complex in mammalian cells (Seaman, 2005). The retromer complex has a conserved structure and function from yeast to mammals. It is composed of five proteins involved in the recycling and retrograde transport of cargo proteins from endosomes to the *trans*-Golgi Network (TGN) (Bonifacino and Rojas, 2006; Seaman, 2005). By searching genome databases, we found that every member of the mammalian retromer complex is conserved in *Arabidopsis thaliana* (Vanoosthuyse et al., 2003). Recently, Oliviusson et al. (2006) showed that three vacuolar protein sorting (VPS) proteins, namely VPS35 (At3g51310), VPS29 (At3g47810), and VPS26 (At5g53530) of the plant retromer complex are localized to multivesicular bodies (MVBs) in tobacco BY2 cells. Additionally, VPS29 is involved in the maturation of the storage proteins 12S globulin and 2S albumin during seed development (Shimada et al., 2006). Nevertheless, the precise function of the retromer complex in cellular trafficking and development in plants remains unknown.

In *A. thaliana*, three genes code for a VPS35 homolog (*At2g17790*, *At1g75850*, and *At3g51310*, which we designated here VPS35a, VPS35b, and VPS35c, respectively), two code for a VPS26 homolog (*At5g53530* and *At4g27690*, which we designated VPS26a and VPS26b, respectively), and only one encodes VPS29 (*At3g47810*). In yeast and animal cells, VPS29 is required for stabilizing

the retromer complex, and *vps29* null mutants exhibit basically the same phenotype as any of the other retromer mutants (Seaman, 2005). Moreover, VPS29 has a phosphoesterase fold, which acts as a protein interaction scaffold for retromer assembly, and exhibits a phosphoesterase catalytic activity in vitro (Collins et al., 2005; Damen et al., 2006; Wang et al., 2005). As only one gene encodes the plant VPS29 protein, we decided to investigate the function of VPS29 by analyzing three *Arabidopsis* null mutant alleles of *vps29*. Here we show that VPS29 is required in many aspects of plant development and is specifically required for proper PIN1 protein cycling downstream of GNOM. Then, we demonstrate that VPS29 is involved in PIN1 repolarization during lateral root formation. Similarly, PIN1 distribution and polarity is affected in *vps29* embryo cells, leading to severe alterations of embryo development. Altogether, our data indicate that SNX1 endosomes and VPS29 play an active role in the formation of new axes of polarity during plant development by mediating trafficking and rerouting of PIN proteins.

RESULTS

Phenotypic Characterization of the *vps29* Mutant in *Arabidopsis*

To study VPS29 function in *A. thaliana*, we analyzed three allelic T-DNA insertion lines in the *VPS29* gene (Figure S1 in the Supplemental Data, available with this article online). The three alleles were null mutants and exhibited the same sporophytic phenotype, which was fully complemented by transgenic expression of a genomic fragment spanning the *VPS29* gene (Figures S1 and S2). These results indicate that *VPS29* is the only gene impaired in the *vps29* mutants.

As previously shown by Shimada et al. (2006), *vps29* plants had a dwarf phenotype compared with wild-type controls (Figure 1A). We found *vps29* seedlings to exhibit abnormal cotyledons in their shape, number, and positioning (Figures 1B–1F, Figures S3 and S4 for quantitative data). Interestingly, the *pin1* single or *pin4 pin7* double mutants have similar defects in cotyledon number and positioning (Benkova et al., 2003). As cotyledons are embryonic leaves, we investigated early embryonic development of *vps29* mutants. In comparison with wild-type controls, the stereotypical pattern of cell division in early embryos was affected in *vps29* mutants (Figures 1G and 1H). In a significant number of *vps29* embryos, the division plan of the apical cell of the embryo was compromised, as demonstrated by horizontal instead of vertical division (Figure 1H). At later stages, mutant embryos continued to exhibit abnormal shapes and cell division defects (see Figure S5 for quantitative data). Here again, the embryo defects in *vps29* were reminiscent of some combinations of *pin* mutants, suggesting a role for VPS29 in regulating PIN protein function during embryogenesis (Blilou et al., 2005; Friml et al., 2003).

Next, we investigated the root phenotype of *vps29*. Seedlings of *vps29* had a reduced primary root length (Figures 1I and 1J) and displayed fewer secondary roots (Figures 1K and 1L) compared with the wild-type. In addition, roots and hypocotyls were agravitropic (Figure 1I). Thus, it appears that VPS29 is required at many stages of embryonic and postembryonic development. Moreover, our data indicate that the *vps29* mutant has phenotypic defects very similar to those of some *pin* mutants.

VPS29 and SNX1 Act in Common Developmental Pathways

To some extent, phenotypic features of *vps29* roots resembled those of *snx1* mutants, although they were less severe in *snx1* (Jaillais et al., 2006). As SNX1 and VPS29 are possible components of the retromer complex in plants, we assumed that they are likely to cooperate in some common developmental pathways. We first quantitatively analyzed the shoot phenotype of two *snx1* single mutant alleles (Figure S6), which had mild defects for both root and shoot development as compared with *vps29*. Then, we crossed the *vps29* and *snx1* mutant lines to examine the genetic interactions between *VPS29* and *SNX1*. In an F3 population derived from the self-pollination of a *VPS29/vps29 snx1/snx1* plant, we found *VPS29/vps29 snx1/snx1* seedlings to show a stronger phenotype than the *snx1* single mutant and harbor cotyledons with aberrant shapes, which was never the case for *snx1* single mutants (Figure 2A and Figure S4). After flowering, *VPS29/vps29 snx1/snx1* plants exhibited an intermediate phenotype between that of *snx1* and *vps29* single mutants (Figure 2B). However, of more than two hundred F3 plants analyzed, we did not find any *vps29/vps29 snx1/snx1* double mutant plants, suggesting that the loss of function of these two genes is either gametophytic or embryonic lethal. Our previous analysis of *snx1* mutants suggested that SNX1 is involved in polar auxin transport in roots (Jaillais et al., 2006). The presence of a genetic interaction between *SNX1* and *VPS29* we detected here indicates that VPS29 is likely to contribute to this pathway, in both the root and the shoot.

As VPS29 is a component of the Vps35-Vps29-Vps26 retromer subcomplex in yeast and mammals, we investigated whether such a retromer subcomplex might occur in plant cells. A two-hybrid screen confirmed the physical interaction between VPS35a and the other two retromer components, VPS26a and VPS29 (Figure 2C). To verify the existence of this subcomplex in plants, we carried out a coimmunoprecipitation experiment using a transgenic line expressing VPS29 fused to the green fluorescent protein (GFP) (Figure 2D). Mass spectrometry analysis revealed the presence of VPS35 and VPS26 isoforms associated with VPS29-GFP in the immunocomplex (Figure S7). Taken together, the genetic interaction between *SNX1* and *VPS29*, the presence of the VPS35-VPS29-VPS26 retromer subcomplex in plants, and the reported degradation of VPS35 in the *Arabidopsis* mutant *vps29-2/mag1-2* (Shimada et al., 2006) suggest that the retromer complex might be involved in the vps29-phenotype.

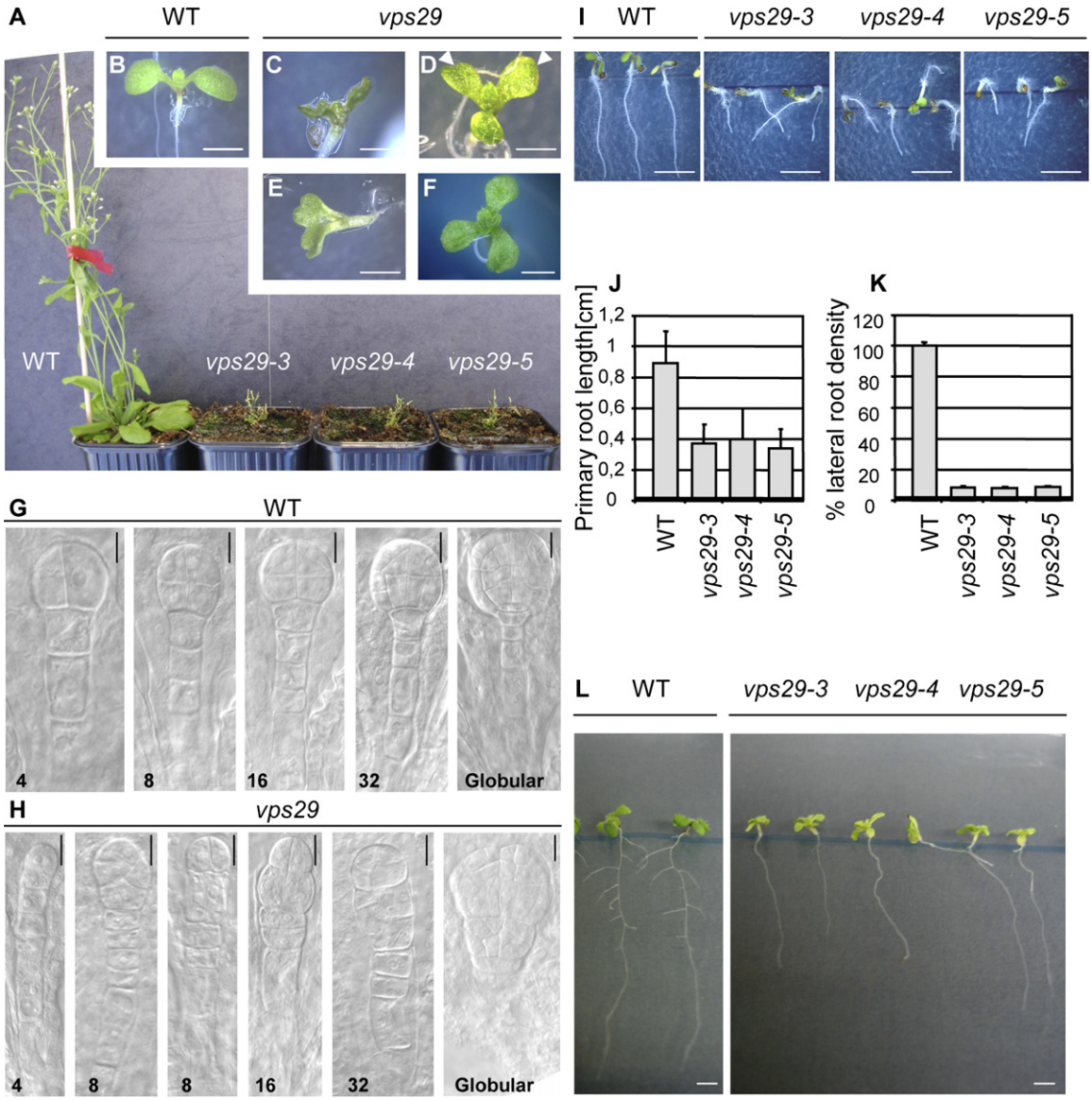

Figure 1. Embryonic and Postembryonic Phenotypes of *vps29* Mutants

(A) Phenotype comparison between wild-type *Arabidopsis* (Col-0) and *vps29-3*, *vps29-4* and *vps29-5* allelic mutants after bolting.

(B–F) Cotyledons of 7-day-old seedlings from the wild-type (B) and *vps29* mutants (C–F). The four phenotypic classes represented in (C)–(F) were observed for the three *vps29* alleles. (C) Small and thick abnormal cotyledons with irregular shape. (D) Abnormal position of cotyledons (arrows). (E) Fusion of cotyledons. (F) Seedling with three cotyledons.

(G and H) Early embryogenesis from the four-cell stage to the globular stage in wild-type (G) and *vps29* embryos (H). Results are representative of the three *vps29* alleles. Figures at bottom left indicate the number of embryo cells.

(I) Primary root and hypocotyl phenotypes of 5-day-old seedlings from the wild-type and *vps29* alleles grown vertically in vitro.

(J) Primary root length of 5-day-old seedlings from the wild-type and *vps29* alleles grown vertically in vitro.

(K) Lateral root density of 15-day-old seedlings from the wild-type and *vps29* alleles grown vertically in vitro.

(L) Secondary root phenotype of 15-day-old seedlings from the wild-type and *vps29* alleles grown vertically in vitro.

Error bars in graphs (J) and (K) indicate SEM. Scale bars, (G) and (H), 5 μm; all others, 5 mm.

The *vps29* Mutant Displays Phenotypes Related to Alteration of PIN1-Mediated Auxin Transport

To determine whether auxin distribution is affected in *vps29*, we used the *DR5rev:GFP* reporter line, which is a reporter of auxin maxima in *Arabidopsis* (Benkova et al., 2003; Friml et al., 2003). In wild-type seedlings, the GFP signal driven by the *DR5* promoter was restricted to the tip of the cotyledons (Figure 3A). In *vps29*, the GFP signal was greatly enhanced in the cotyledon tip and extended to the vascular tissue and margins of cotyledons

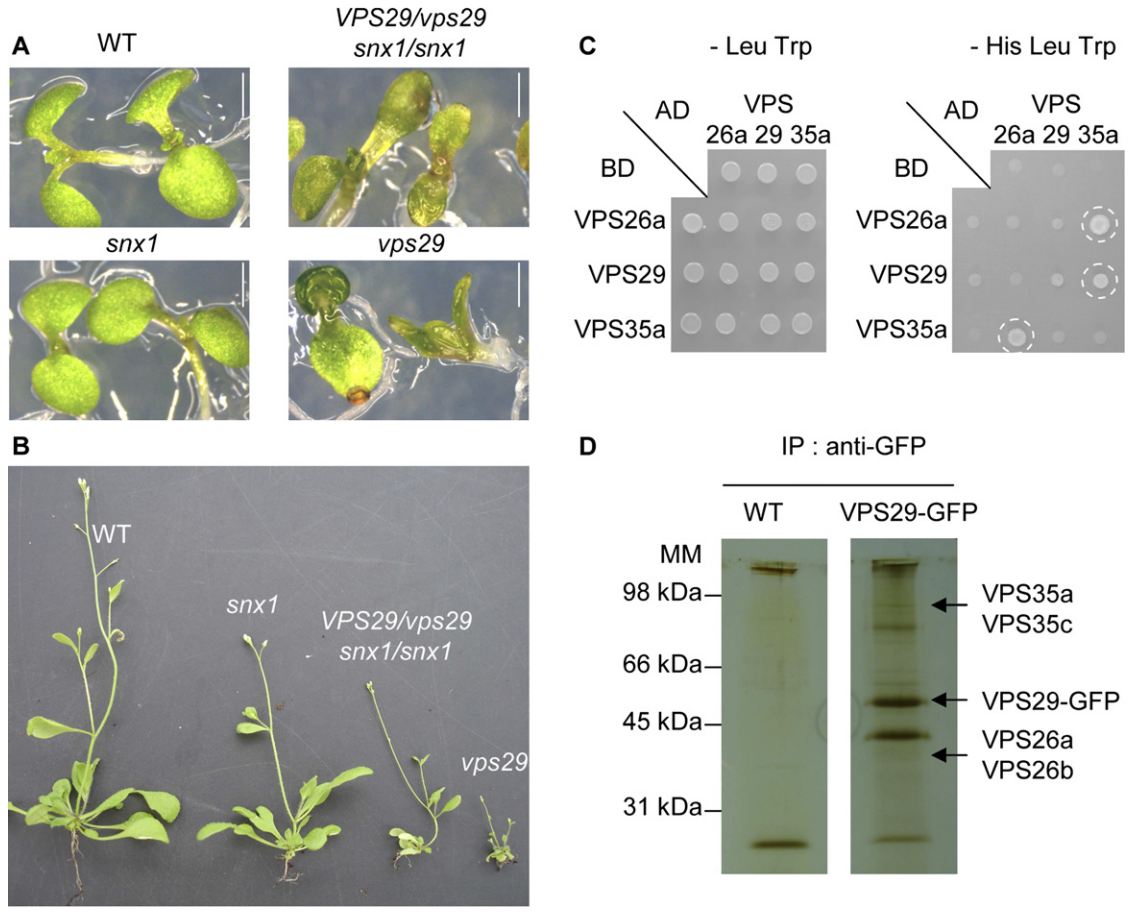

Figure 2. Interaction between VPS29 and Other Plant Retromer Proteins

(A) Cotyledon phenotypes of the wild-type, *snx1* single mutant, *vps29* single mutant, and *VPS29/vps29 snx1/snx1* mutant.

(B) Phenotype of the wild-type, *snx1*, *vps29*, and *VPS29/vps29 snx1/snx1* plants after bolting.

(C) Yeast two-hybrid analysis of the binary interactions between components of the VPS35-VPS29-VPS26 retromer subcomplex. VPS35a, VPS26a, and VPS29 were used as either bait or pray. AD, activation domain; BD, binding domain. Dashed circle labeles positive interactions.

(D) Silver-stained SDS-PAGE of the VPS29-GFP immunocomplex after immunoprecipitation of wild-type and VPS29-GFP-expressing leaves. Molecular mass (MM) markers are indicated on the left.

In (A) and (B), phenotypes are representative of different allelic combinations. Scale bars, 5 mm.

(Figure 3A). In contrast, the *DR5* reporter was less active at the primary root tip of *vps29* than in the wild-type control (Figure 3B). Next, we asked whether sensitivity or response to auxin (or both) are altered in roots of the *vps29* mutant. We treated roots with the transportable 1-Naphtalene-Acetic-Acid (NAA) auxin analog, which is known to artificially induce secondary root formation throughout the whole pericycle (Benkova et al., 2003). In *vps29*, we observed that poorly defined secondary root primordia were induced by NAA treatment (Figure 3C). This result indicates that *vps29* is capable of sensing auxin treatment and subsequently initiating lateral root primordia, but is unable to produce fully polarized lateral roots. Similar results were observed in *pin3 pin7* and *pin1 pin3 pin4* mutants (Benkova et al., 2003). Control of auxin transport by PIN1 is known to be crucial for vascular tissue development (Galweiler et al., 1998). In wild-type shoots, vascular tissue forms individual bundles (Figure 3D), which are partially fused in *pin1* mutant and shows abnormal xylem proliferation (Galweiler et al., 1998). Shoots of *vps29* exhibited xylem overproliferation and a continuous xylem strand consisting of xylem poles fused to interfascicular parenchyma that differentiated into xylem (Figure 3D and Figure S8 for a more detailed analysis). As in *pin1*, phloem poles remained well separated and no overproliferation of phloem was detected. Altogether, our results suggest that *vps29* has altered PIN function in polar auxin transport.

To explore this hypothesis, we investigated the genetic interaction between *vps29* and the *pin1* auxin efflux carrier mutant. We chose *pin1* because vps29-phenotypes resemble those of *pin1* in many aspects, with the notable exception of the characteristic pin-formed inflorescent shoot apical meristem (SAM) phenotype (Galweiler et al., 1998). We found all seedlings generated from self-pollination of

a *vps29/vps29 PIN1/pin1* plant to exhibit a vps29-phenotype, meaning that *vps29 pin1* double mutant seedlings cannot be distinguished from *vps29* single mutant plants (Figure 3E and Figure S4). This result is consistent with a role for VPS29 in regulating PIN1 function during seedling development. After flowering, *vps29 pin1* double mutant plants had an additive phenotype reflecting the sum of the two single mutant phenotypes; the plants were dwarf with a pin-shaped shoot (Figure 3F). This suggests that VPS29 does not control PIN1 function in the inflorescence SAM.

This could be explained if *VPS29* is not expressed in the inflorescence SAM, where *PIN1* is active (Vernoux et al., 2000). To test this assumption, we checked the expression pattern of *VPS29* by in situ hybridization and by analyzing *VPS29:VPS29-GUS*-expressing lines. *VPS29* transcripts were not detected in the SAM but were found in older organs and in flowers (Figure 3G and Figure S9). As PIN1 acts in the SAM to regulate organ formation and phyllotaxis in the shoot, this result explains why the *vps29* single mutant did not display a pin-shaped-phenotype. Thus, it appears that VPS29 is a major mediator of PIN1 function during root, vascular tissue, and seedling development, where both VPS29 and PIN1 are expressed (Figure S9 and Benkova et al., 2003; Galweiler et al., 1998), but is not involved in organ initiation at the SAM, where only PIN1 is expressed (Vernoux et al., 2000).

Another regulator of PIN1 function is the protein kinase PINOID (PID) (Christensen et al., 2000). *pid* and *pin1* single mutant phenotypes are very similar in both seedling and shoot development (Furutani et al., 2004). To address whether VPS29 and PID act in the same developmental pathways, we generated *vps29 pid* double mutants. *vps29 pid* seedlings showed a strong synergistic phenotype compared with the phenotype of single mutants (Figure 3E). Double mutant seedlings totally lacked cotyledons (Figure 3E) but had a functional SAM capable of generating leaves. However, leaves were often fused and formed a radial cup surrounding the SAM (Figure S10). Interestingly, similar phenotypes were reported for *pin1 pid* double mutants (Furutani et al., 2004) (see Figure 3E and Figure S10). In the *vps29 pid* double mutant, *vps29* mimics the defect provided by the loss of function of *PIN1* in the *pin1 pid* double mutant. These results strongly argue for a role for VPS29 in regulating PIN1 function during seedling development.

Altogether, our data indicate that VPS29 is required for the establishment of normal *DR5* maxima in cotyledons and roots, and that some features of the vps29-phenotype can be explained by alteration of PIN1 function.

VPS29 Is Localized to SNX1 Endosomes

In tobacco BY2 cells, VPS29 colocalizes with two other retromer components, VPS35 and VPS26, and with vacuolar sorting receptor-1 (VSR1) at the surface of MVBs (Oliviusson et al., 2006). To ascertain the subcellular localization of VPS29 in intact *Arabidopsis* root apices, we used the same genomic construct as that for the complementation experiment, but we added the coding sequence of the *GFP* at the 3′ end (Figure S2). This construct was functional; it can fully rescue the *vps29* mutant (Figure S2). We analyzed VPS29-GFP localization in living *Arabidopsis* roots and found the fusion protein to label punctate structures in the cytosol (Figure 4A). VPS29-GFP-labeled compartments were sensitive to both Wortmannin (Wm) (Figure 4B) and Brefeldin A (BFA) (Figures 4C–4E), which are two drugs that alter endosomes (Jaillais et al., 2006). Additionally, VPS29-GFP-labeled compartments were stained by the FM4-64 endocytic tracer after 15 min of dye treatment (Figures 4F–4H). Next, we crossed the *VPS29:VPS29-GFP*-expressing line with either a *35S:mRFP-RABF2b* or a functional *SNX1:SNX1-mRFP* expressing line, which are both endosome marker lines (Jaillais et al., 2006; Takano et al., 2005). In hybrid seedlings, we detected a strong colocalization between VPS29-GFP and mRFP-RABF2b (Figures 4I–4K) or SNX1-mRFP (Figures 4L–4N). In contrast, VPS29 did not colocalize with the Golgi, TGN, or GNOM endosome markers in root cells (Figure S11). Altogether, our localization study indicates that VPS29 is localized to SNX1 endosomes in *Arabidopsis* roots.

VPS29 Is Required for Maintaining SNX1 Endosome Morphology

Next, we investigated the impact of *VPS29* loss of function on the morphology of endosomal compartments. In *vps29*, both GFP-RABF2b and SNX1-GFP markers were found in aberrant enlarged endosomes (Figures 5A–5D). To determine whether *VPS29* loss of function affects SNX1 endosomes specifically, we introgressed a *GNOM:GNOM-GFP* or *VHA-a1:VHA-a1-GFP* reporter line in the *vps29* mutant (Dettmer et al., 2006; Geldner et al., 2003). GNOM-GFP compartments, as well as the TGN labeled with VHA-a1-GFP, had a normal shape and size in *vps29* (Figures 5E–5H). The Golgi apparatus markers ERD2-GFP and ST-GFP were also not disturbed in *vps29* roots (Figure S12). In addition, GNOM-GFP- and VHA-a1-GFP-labeled compartments displayed the same BFA sensitivity in *vps29* as in wild-type plants (Figures 5M–5P). Both markers accumulated inside the so-called "BFA compartment" together with internalized FM4-64 after BFA treatment. Interestingly, this was not the case for GFP-RABF2b- and SNX1-GFP-labeled endosomes, which still accumulated in BFA compartment, but were basically not stained by endocytosed FM4-64 in *vps29*, contrary to the wild-type (Figures 5I–5L). Together these data indicate that VPS29 is required to maintain the normal morphology and homeostasis of SNX1 endosomes, whereas it is not necessary to preserve the integrity of GNOM endosomes.

VPS29 Is Specifically Required for PIN1 and PIN2 Trafficking

As VPS29 is needed for both maintaining SNX1 endosome homeostasis and regulating PIN1 function, we investigated whether VPS29 is involved in PIN endocytic trafficking. In roots of a *pin1* mutant line complemented by the

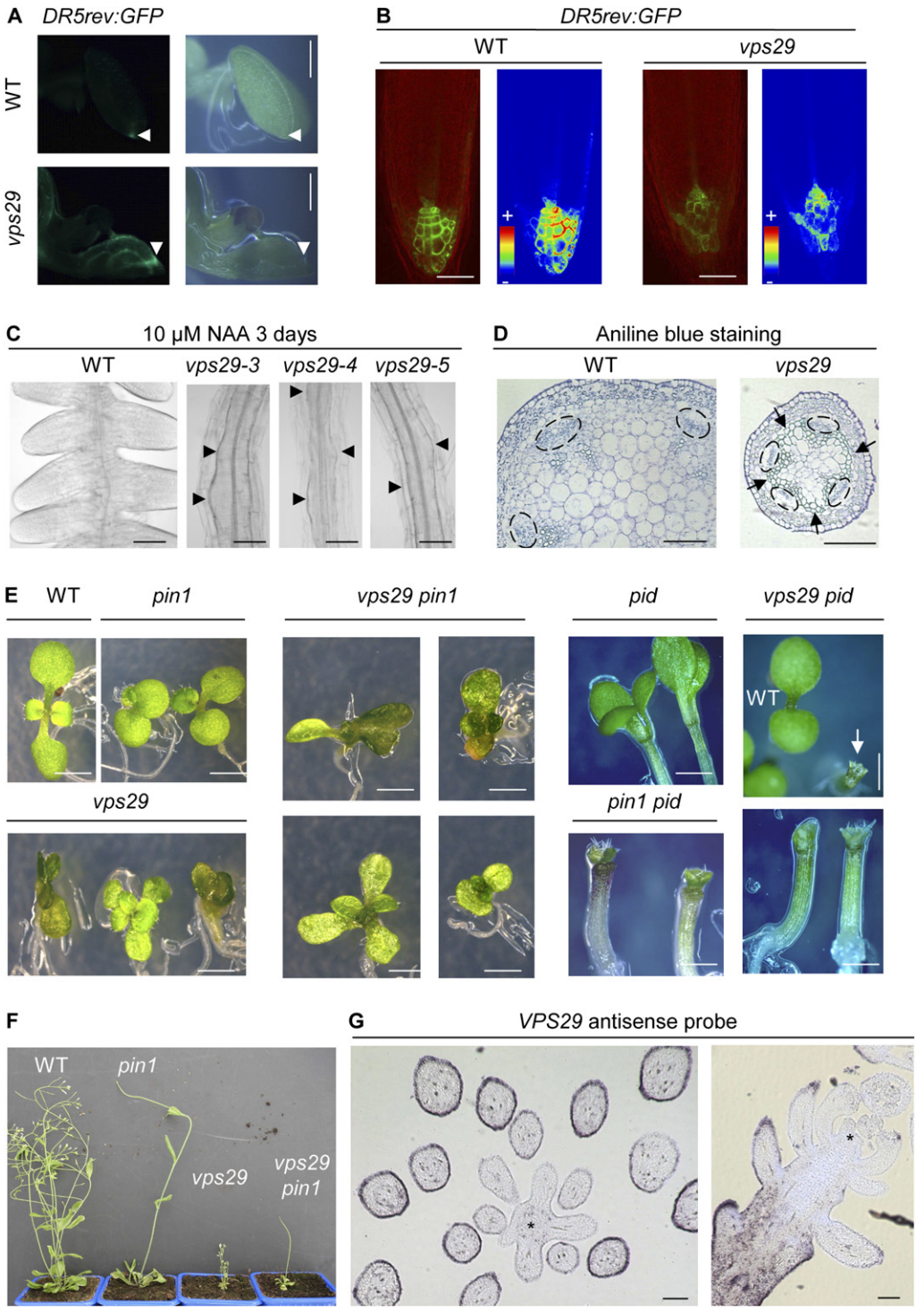

Figure 3. *vps29* Has Auxin-Related Phenotypes

(A) *DR5rev:GFP* expression pattern in wild-type and *vps29* cotyledons. Left, GFP channel; right, white light. Arrowheads indicate cotyledon tips.

(B) *DR5rev:GFP* expression pattern in the wild-type and *vps29* primary root. Left, GFP channel; right, color-coded signal intensity (from blue, low signal, to red, high signal).

(C) Induction of lateral root development after NAA treatment of wild-type and *vps29* mutant roots. Arrowheads indicate primordia in *vps29* alleles.

(D) Aniline blue staining of stem cross-sections in wild-type and *vps29* mutant plants. Individual phloem poles are circled by a dashed line and extra-xylem in the interfascicular space is indicated by arrows in *vps29*.

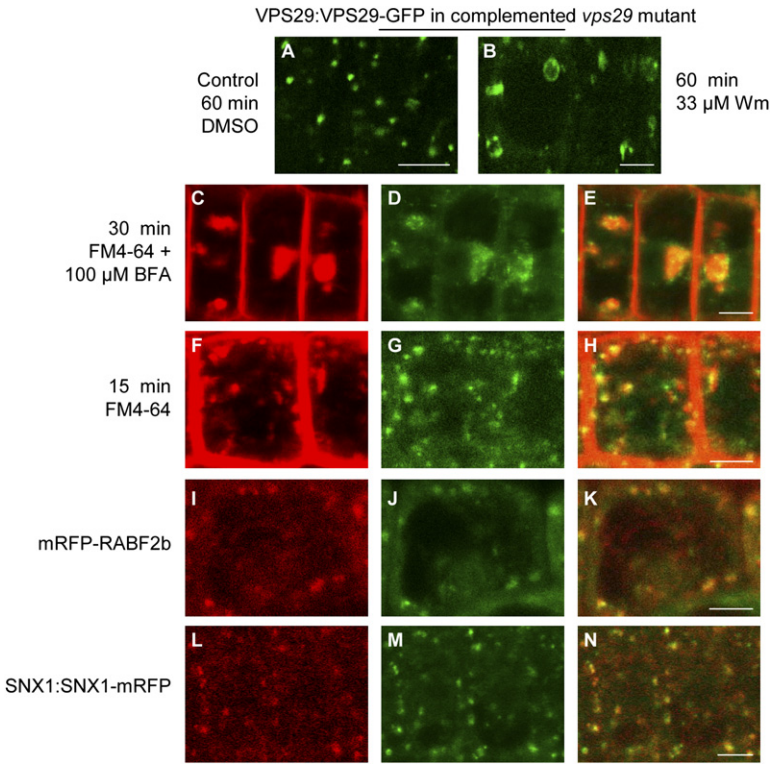

Figure 4. VPS29 Is Localized in SNX1 Endosomes

(A and B) VPS29-GFP labeling in root cells of the complemented *vps29* mutant. (A) Mock treatment, (B) after Wortmannin treatment.

(C–E) BFA sensitivity of the VPS29-GFP-labeled compartment in the presence of the endocytic tracer FM4-64. (C), FM4-64, (D), VPS29-GFP, and (E), merge.

(F–H) Colocalization of FM4-64 and VPS29-GFP. (F), FM4-64, (G), VPS29-GFP, and (H), merge.

(I–K) Hybrid seedlings coexpressing *mRFP-RABF2b* and *VPS29:VPS29-GFP*. (I), mRFP-RABF2b, (J), VPS29-GFP, and (K), merge.

(L–N) Hybrid seedlings coexpressing *SNX1:SNX1-mRFP* and *VPS29:VPS29-GFP*. (L), SNX1-mRFP, (M), VPS29-GFP, and (N), merge.

Scale bars, 5 μm.

PIN1:PIN1-GFP construct, PIN1-GFP was basally localized at the PM of stele cells (Figure 6A) (Benkova et al., 2003). In *vps29*, although PIN1-GFP remained properly basally localized at the PM, it also accumulated within aberrant enlarged compartments in stele cells (Figure 6B). As we previously showed that SNX1 endosomes are enlarged in *vps29*, we hypothesized that PIN1-GFP is blocked in these enlarged SNX1-labeled compartments. To check this assumption, we introduced both PIN1-GFP and SNX1-mRFP markers into *vps29*. Intracellular PIN1-GFP labeling accumulated with SNX1-mRFP in the enlarged compartments in *vps29* (Figure S13). To ascertain that PIN1 localization was not artifactually caused by the GFP tag, we looked directly at the localization of endogenous PIN1 proteins in *vps29* by using a specific anti-PIN1 antibody. We found endogenous PIN1 to accumulate in large intracellular compartments in *vps29*, confirming that routing of PIN1 is affected in *vps29* (Figure S14).

We then wondered whether PIN2, which is also expressed in root apex, might be mislocalized in *vps29* as well. To address this question, we introgressed a *PIN2:PIN2-GFP* transgenic line into the *vps29* background (Xu and Scheres, 2005b). PIN2 is apically localized in epidermal cells, whereas it is basally localized in cortical cells (Figure 6C) (Blilou et al., 2005). In *vps29*, PIN2-GFP was properly polarized at the PM, but it also accumulated within the characteristic enlarged intracellular compartments of *vps29* root cells (Figure 6D and Figure S13). However, intracellular accumulation of PIN2 was less pronounced than that observed for PIN1. Next, we used the same strategy to analyze the role of VPS29 in the trafficking of other PM proteins such as AUX1, low temperature inducible protein 6b (LTi6b), and plasma membrane intrinsic protein 2a (PIP2a) (Cutler et al., 2000; Swarup et al., 2004). Interestingly, AUX1-YFP, GFP-LTi6b, and GFP-PIP2a remained correctly localized to the PM and were not found to label enlarged intracellular compartments in *vps29* (Figures 6E–6J). Altogether, our results show that VPS29 is involved in the trafficking of at least two PIN proteins in root cells. Moreover, the protein trafficking pathway mediated by VPS29 appears to be specific to some cargo proteins, since AUX1, LTi6b, and PIP2a localization seems to be independent of a functional VPS29. We cannot exclude the possibility that VPS29 might be involved in the routing of cargos other than PIN1 and PIN2. Thus, it is possible that some of the vps29-phenotypes we reported here might be unassociated with alterations of auxin transport and PIN function.

(E) Cotyledon phenotypes of the wild-type, *pin1* single mutant, *vps29* single mutant, *vps29 pin1* double mutant, *pid* single mutant, and *pin1 pid* and *vps29 pid* double mutants. The arrow indicates the *vps29 pid* double mutant seedling.

(F) Phenotype of the wild-type, *pin1*, *vps29*, and *vps29 pin1* plants after bolting.

(G) *VPS29* expression pattern in the wild-type inflorescence after in situ hybridization on transversal (left) and longitudinal (right) sections. *VPS29* transcripts are not present in the shoot apical meristem (asterisk) but are expressed in older organs.

These experiments were performed in at least two *vps29* alleles. Scale bars in (A) and (E), 5 mm; (B) and (C), 20 μm; and (D) and (G), 100 μm.

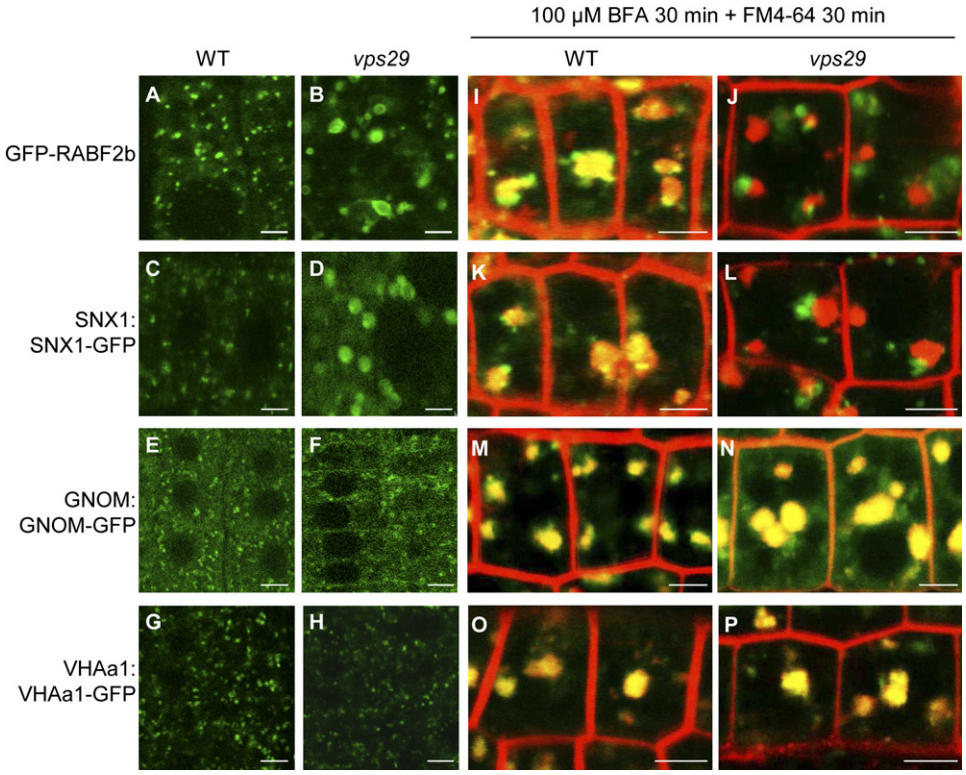

Figure 5. VPS29 Controls SNX1 Endosome Morphology

(A and B) GFP-RABF2b localization in wild-type (A) and *vps29* (B) roots. Note the aberrant size of GFP-RABF2b-labeled compartments in *vps29* compared with the wild-type.

(C and D) SNX1-GFP localization in wild-type (C) and *vps29* (D) roots.

(E and F) GNOM-GFP localization in wild-type (E) and *vps29* (F) roots. Note that GNOM-GFP-labeled compartments are similar in size in wild-type and *vps29* roots.

(G and H) VHA-a1-GFP localization in wild-type (G) and *vps29* (H) roots.

(I–P) Effects of BFA on endosomes and the TGN in wild-type and *vps29* roots. Wild-type (I, K, M, and O) or *vps29* (J, L, N, and P) seedlings were treated with BFA and FM4-64. Endosome markers are GFP-RABF2b (I and J), SNX1-GFP (K and L), and GNOM-GFP (M and N), whereas the TGN marker is VHA-a1-GFP (O and P).

These experiments were performed at least in two *vps29* alleles. Scale bars, 5 μm.

VPS29 Is Required for Efficient PIN1 Cycling Downstream of GNOM

Accumulation of PIN1 into enlarged intracellular compartments led us to ask whether it is PIN1 recycling toward the PM or its degradation that is affected in *vps29*. To distinguish between these two possibilities, we studied *PIN1:PIN1-GFP*-expressing seedlings in wild-type and *vps29* backgrounds after treatment with cycloheximide (CHX), a protein synthesis inhibitor. In the wild-type background, PIN1-GFP remained properly localized at the PM after 4 hr of CHX treatment, and we noticed almost no decrease in the GFP signal (Figure 6K). In contrast, PIN1-GFP labeling disappeared almost completely in *vps29*, especially at the PM (Figure 6L). This experiment indicates that PIN1 degradation is not compromised in *vps29*, while its recycling is likely to be altered. This implies that in the absence of recycling, PIN1 is sent for degradation by a default pathway. To gain more direct clues as to whether PIN1 cycling is indeed affected in *vps29*, we performed a fluorescence recovery after photobleaching (FRAP) analysis. In the control experiment, we observed a recovery of PIN1-GFP at the PM of stele cells within 20 to 30 min after photobleaching (Figure 6M and Figure S15 for quantitative data). This recovery was largely delayed either when recycling in wild-type was blocked by BFA treatment or in the *vps29* mutant (Figures 6N and 6O, and Figure S15). Thus, PIN1-GFP recovery at the basal side of the PM is conditioned by endocytic recycling, is dependent on the GNOM BFA-sensitive pathway, and involves the VPS29 protein.

As both GNOM and VPS29 are required for PIN1 recycling, we next investigated whether VPS29 acts upstream or downstream of GNOM. As GNOM is the only BFA-sensitive ARF-GEF required for PIN1 recycling (Geldner et al., 2003), we looked at the effect of BFA on PIN1-GFP localization in roots of the wild-type and *vps29* mutant. While PIN1-GFP accumulated in FM4-64-labeled BFA compartment in wild-type roots, we detected PIN1-GFP in two subcompartments in *vps29*; one displayed only a green

fluorescent signal, whereas the other exhibited a yellow fluorescent signal corresponding to the sum of GFP and FM4-64 fluorescence (Figure 6P). Because we previously showed that SNX1-GFP endosomes form a compartment distinct from FM4-64-labeled, GNOM-GFP endosomes upon BFA treatment in *vps29* background (Figures 5I–5N), we can assume that the GFP-labeled compartment corresponds to SNX1 endosomes, while the other corresponds to GNOM-endosomes. This observation suggests that BFA blocked trafficking of PIN1-GFP from GNOM toward SNX1 endosomes (Figure 6Q). Altogether, these data suggest that PIN1 is internalized first through GNOM endosomes and is then routed to SNX1 endosomes for its recycling to the PM.

VPS29 Mediates Change of PIN1 Polarity during Development

In *vps29,* PIN1 remains basally localized in the stele cells, indicating that VPS29 is not required for maintaining PIN1 polar localization in these cells. However, because of the severe effects of the loss of function of *VPS29* on seedling development, we asked whether VPS29 could be involved in the control of PIN1 polarity during some developmental processes. For that purpose, we first looked at *vps29* embryos, as control of PIN1 polarity is essential for proper embryo development (Benkova et al., 2003; Friml et al., 2003). In *vps29* embryos exhibiting a wild-type-like morphology (about 40% of *vps29* embryos, see Figure S5), we found that PIN1 polarity failed to establish properly in some cells (Figures 7E–7H) compared with the stereotypical pattern of PIN1 polarity in wild-type embryos (Figures 7A–7D). In *vps29* embryos with abnormal shape (about 60% of *vps29* embryos, see Figure S5), PIN1 polarity and localization were more dramatically affected (Figures 7I–7L). In these embryos, PIN1 polarity was no longer coordinated and PIN1 accumulated inside the *vps29* enlarged intracellular compartments (Figure 7L). This mislocalization of PIN1 was associated with altered auxin maxima, as deduced by *DR5rev:GFP* expression levels (Figure S16).

Next, we examined PIN1 polarity during lateral root emergence, as lateral root formation is strongly affected in *vps29* (Figure 1). In the wild-type, at very early stages of secondary root formation, PIN1-GFP was found at the basal side but also at the lateral side of the cells, facing the new root apex (Figures 7M and 7N). Later, nearly all the cells of the emerging primordia displayed laterally polarized PIN1 (Figure 7N). In *vps29* young lateral root primordia, PIN1-GFP labeling was found at the PM and within the intracellular enlarged compartments (Figures 7O and 7P). Interestingly, at every stage of early lateral root development, lateral repolarization of PIN1-GFP failed and PIN1-GFP remained almost exclusively at the basal side of the cells (Figure 7P). As in embryos, the mislocalization of PIN1 was associated with an altered auxin maximum (Figure S16). This result indicates that VPS29 is required for the reorientation of PIN1 polarity during secondary root formation and the establishment of new root primordia. Thus, VPS29 is involved in PIN1 polarity rearrangement and coordination during both embryo and root development.

Small GTPases of the Rho of Plant (ROP) family are known to be regulators of cell polarity in different cell systems (Xu and Scheres, 2005a). Interestingly, overexpression of a constitutive active (CA)-ROP2 leads to increased lateral root formation (Li et al., 2001), suggesting that ROP2 and VPS29 might be involved in the same developmental pathway. Thus, we examined the lateral root phenotype in *vps29* plants overexpressing CA-ROP2. These plants displayed the same phenotype as the *vps29* single mutant, characterized by a very limited number of lateral roots (Figure S17). This indicates that VPS29 is required for ROP2 function in lateral root emergence.

DISCUSSION

A Retromer Complex in *Arabidopsis*

Here, we show that VPS29 is a component of the VPS35-VPS29-VPS26 retromer subcomplex in plants. Interestingly, we found *SNX1* and *VPS29* to interact genetically. This implies that both proteins play a part in the regulation of common developmental pathways. This result is particularly interesting when compared to the similar genetic interactions that occur between SNX and retromer components in mammals (Griffin et al., 2005). Indeed, while *Snx1* and *Snx2* single knockout mice have no apparent phenotype, development of $Snx2^{-/-}Vps26^{+/-}$ embryos is severely impaired (90% lethality), which gets even worst in $Snx1^{+/-}$ background (100% lethality for $Snx1^{+/-}Snx2^{-/-}Vps26^{+/-}$ embryos). In our analysis, we failed to generate *vps29 snx1* double mutants, indicating that the two retromer proteins SNX1 and VPS29 are essential for gametophyte or seedling survival. Whether VPS29 plays specific functions independently of the other retromer proteins, or whether the vps29-phenotype we described here basically reflects the function of the entire retromer complex, remains to be elucidated.

Endocytic Recycling of PIN1 Is Required for PIN1 Repolarization during Development

Recently, Sauer et al. (2006) suggested that the ARF-IAA pathway is required to induce the expression of genes involved in PIN1 lateralization during secondary root formation. Here, we have identified VPS29 as a protein that mediates the dynamic rearrangement of PIN1 during developmental processes, including embryo development and formation of secondary roots. By searching microarray databases, we found that the *VPS29* gene, as well as all the other genes encoding retromer components, is not induced by auxin or auxin transport inhibitor treatments (Figure S18). Thus, it is likely that *VPS29* is not one of the cellular effectors induced by the ARF-IAA pathway.

We may hypothesize that VPS29 is constitutively present in root cells, whereas some unknown components of the PIN1 lateralization machinery are missing. Thus, in

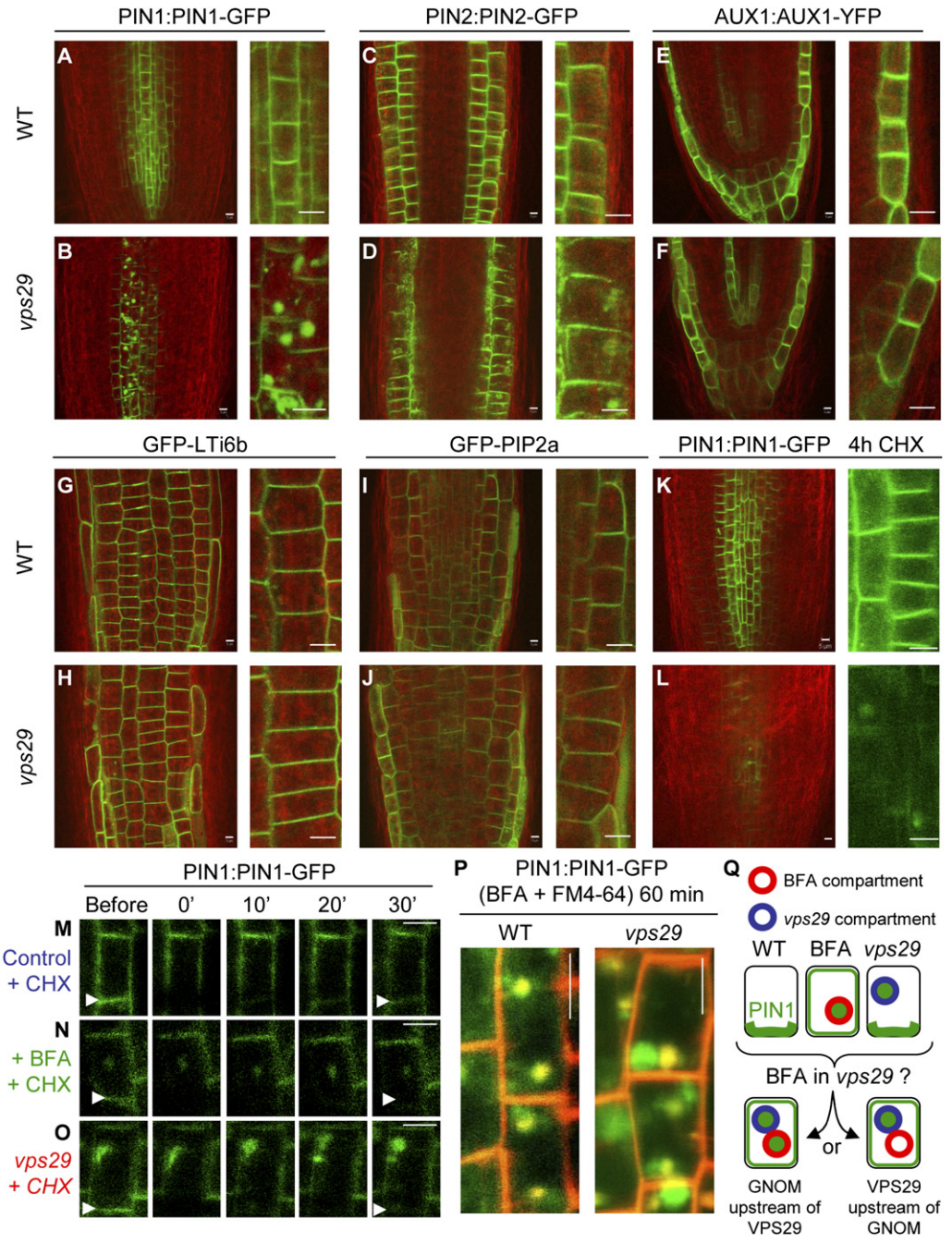

Figure 6. VPS29 Mediates PIN1 and PIN2 Cycling

(A and B) PIN1-GFP localization in wild-type (A) and *vps29* (B) roots. Note (enlargements at the right) that PIN1 remains localized at the PM but also accumulates inside an aberrant intracellular compartment in *vps29*.

(C and D) PIN2-GFP localization in wild-type (C) and *vps29* (D) roots. Note (enlargements at the right) that PIN2 remains localized at the PM but also accumulates, although to a lesser extent, inside an aberrant intracellular compartment in *vps29*.

(E and F) AUX1-YFP localization is identical in wild-type (E) and *vps29* (F) roots.

(G and H) GFP-LTi6b localization is identical in wild-type (G) and *vps29* (H) roots.

(I and J) GFP-PIP2a localization is identical in wild-type (I) and *vps29* (J) roots.

(K and L) PIN1-GFP localization after four hours of CHX treatment in wild-type (K) and *vps29* (L) roots. Note that PIN1-GFP is almost totally degraded in *vps29*.

(M–O) FRAP analysis of PIN1-GFP dynamics. Seedlings were treated 1 hr in CHX prior to the experiment. (M) CHX-treated wild-type root, (N) CHX- and BFA-treated wild-type root, (O) CHX-treated *vps29* root.

(P) PIN1-GFP (green) and FM4-64 (red) localization in wild-type and *vps29* roots after 60 min of 100 μM BFA treatment.

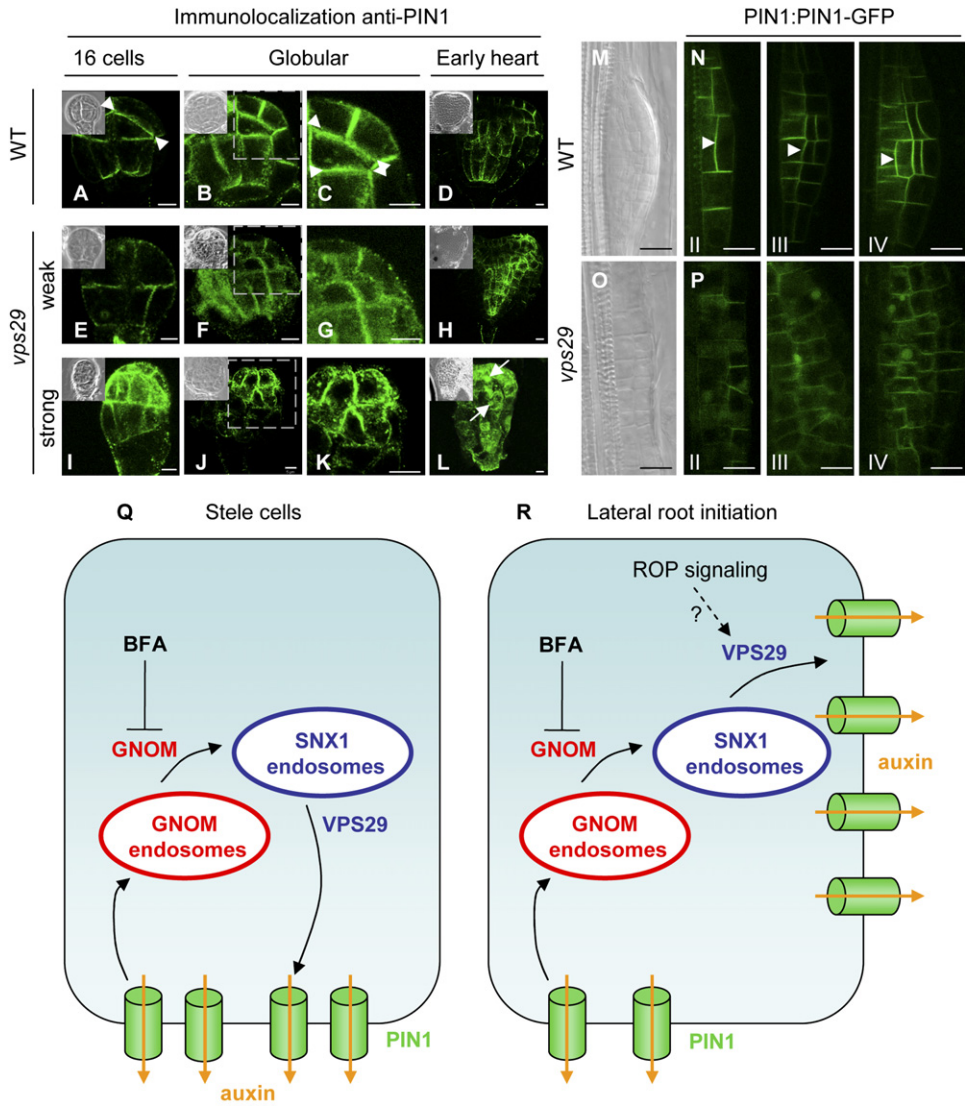

Figure 7. VPS29 Controls Change of PIN1 Polarity during Development

(A–L) PIN1 immunolocalization in wild-type embryos (A–D) and *vps29* embryos with mild defects (E–H) and strong defects (I–L). (C, G, and K) enlargements of (B), (F), and (J). 16 cells, Globular, and Early heart indicate embryo developmental stages. Insets, DIC images. Arrowheads indicate polar localization of PIN1 in wild-type embryo cells, and arrows indicate internalized PIN1. (M and O) Secondary root primordia in the wild-type (M) and *vps29* (O) after NAA treatment. (N and P) PIN1-GFP localization in wild-type (N) and *vps29* (P) primordia during development. Arrowheads show lateral polar localization of PIN1-GFP in the wild-type. We performed this experiment either with or without lateral root induction by 10 μM NAA and obtained the same results. II–IV, lateral root developmental stages. (Q and R) A two-step model for PIN1 cycling in primary roots (Q) and during lateral root initiation (R).

These experiments were performed in at least two *vps29* alleles. Scale bars in (A)–(L), 5 μm, and (M)–(P), 10 μm.

the absence of auxin accumulation, PIN1 remains basally localized in stele cells. When auxin levels increase, the ARF-IAA pathway is induced and leads to the expression of a variety of proteins including those required for PIN1 lateralization. These latter proteins would cooperate with the VPS29 pathway to mediate change in PIN1 polarity.

In cells of *gnom* or *vps29* embryos, although recycling of PIN1 is strongly altered, PIN1 remains polarized at the cellular level. However, PIN1 polarization is not coordinated from cell to cell in the mutant embryos (Steinmann et al., 1999). This observation suggests that endocytic recycling is not required for the maintenance of PIN1 polarity at the

(Q) Schematic representation of (P) indicating the two possible alternatives for BFA action in *vps29*.

These experiments were performed in at least two *vps29* alleles. Scale bars, 5 μm.

cell level, but is likely to be essential for the establishment of a coordinated PIN1 polarity between cells.

We propose that the continuous cycling of PIN proteins is a constitutive pathway that allows rerouting of PIN proteins toward a target compartment, such as (in the case of PIN1) the lateral side of the cell (Figures 7Q and 7R). Our experimental data support a two-step model for PIN1 trafficking. Following PIN1 internalization, PIN1 is routed first toward the GNOM endosomes and then to the SNX1 endosomes for sorting. Trafficking between GNOM and SNX1 endosomes is mediated by GNOM, while that between SNX1 endosomes and the PM involves VPS29. The sorting decision that occurs at the endosomal level would be triggered by developmental or environmental cues. As a functional VPS29 is required for CA-ROP2 activity during lateral root formation (Figure S17), and as ROPs have been involved in the control of cell polarity and the auxin pathway (Lavy et al., 2007; Tao et al., 2002; Xu and Scheres, 2005a), VPS29 and ROPs might work in concert to mediate PIN repolarization and cell polarity (Figure 7R). In conclusion, endosomes provide a dynamic platform that is used for rerouting PIN proteins to new cellular compartments.

A Role for the Plant VPS29 in the Selective Cycling of Some PM Proteins

In yeast, the retromer complex is involved in the retrograde transport of cargo proteins, such as the intracellular sorting receptor Vps10, from endosomes to the TGN (Seaman, 2005). This function is conserved in animals; the loss of function of VPS26, VPS29, VPS35, or both SNX1 and SNX2 inhibits the retrograde transport of the cation-independent mannose 6 phosphate receptor (CiM6PR) from endosomes to the TGN (Bonifacino and Rojas, 2006; Seaman, 2005). In plants, recent data strongly suggest that the retromer complex has conserved this function of mediating retrograde trafficking (Oliviusson et al., 2006; Shimada et al., 2006). In the present work, we show that VPS29 is involved in the cycling of certain PM proteins and is required for the establishment of cell polarity during some developmental processes in plants. To our knowledge, a function of the retromer complex in mediating cell polarity during development of multicellular organisms has never been reported so far. It is worth noting that the mammalian VPS35-VPS29-VPS26 retromer subcomplex has been involved in transcytosis of the polymeric immunoglobulin receptor in polarized epithelial cells (Verges et al., 2004). These data indicate that the retromer components of eukaryotic organisms have evolved additional functions compared with those of yeast retromer, such as recycling of specific cargos from endosomes to the PM.

In animal development, secreted Wnt proteins act as morphogens that are involved in patterning of the developing embryo by forming long-range concentration gradients along the anteroposterior axis (Coudreuse and Korswagen, 2007). In *Caenorhabditis elegans* and vertebrates, the function of the retromer has recently been shown to be required for the establishment of this gradient by the Wnt-producing cells (Coudreuse et al., 2006; Prasad and Clark, 2006). When retromer function is impaired, Wnt gradient is absent and severe defects in the organization of the anteroposterior axis are observed. The canonical function of the retromer has been proposed to be involved in proper Wnt signaling, through the regulation of the retrograde transport of a putative Wnt cargo receptor from the endosomes to the TGN in Wnt-expressing cells. However, this remains entirely speculative because Wnt trafficking has not been analyzed at the intracellular level. It is therefore attractive to imagine another function for the animal retromer that would be similar to that displayed by the plant VPS29 retromer protein in mediating cargo trafficking from the endosomes to the plasma membrane. Further studies are obviously required to understand the exact role of the retromer in Wnt signaling and whether a function of the retromer for protein cycling from endosomes to the PM might have been conserved between plants and animals.

EXPERIMENTAL PROCEDURES

Materials and Growth Conditions

The *vps29-3* (Columbia accession, SALK010106), *vps29-5* (Columbia accession, SALK117264) and *vps29-4* (Columbia accession, GABI125H09) T-DNA mutant lines were obtained from the SALK Institute (Alonso et al., 2003) and Bernd Weisshaar (MPI for Plant Breeding Research; Cologne, Germany), respectively. The *snx1-1*, *snx1-2*, *pin1-6*, *pid14*,and *pin1 pid* mutant lines, the *GNOM:GNOM-GFP* line in *gnom* background, *PIN1:PIN1-GFP* line in *pin1* background, *PIN2:PIN2-GFP* line in *pin2* (*eir1-1*) background, *SNX1:SNX1-mRFP* line in *snx1-1* background, *SNX1:SNX1-GFP* line in *snx1-1* background, *VHA-a1:VHA-a1-GFP* line in *vha-a1* background, *AUX1:AUX1-YFP*, *35S:GFP-LTi6b*, *35S:GFP-PIP2a*, *35S:GFP:RABF2b*, *35S:mRFP-RABF2b*, and *DR5rev:GFP* lines were described previously (Benkova et al., 2003; Cutler et al., 2000; Dettmer et al., 2006; Friml et al., 2003; Furutani et al., 2004; Geldner et al., 2003; Jaillais et al., 2006; Swarup et al., 2004; Takano et al., 2005; Xu and Scheres, 2005b). Plants were grown in soil with long daylight at 21°C and 70% humidity. For root analysis, seedlings were grown vertically on MS medium in Petri dishes for the indicated period of time. NAA treatments were performed as described (Benkova et al., 2003; Sauer et al., 2006).

For double mutant analysis, two to three allelic combinations were analyzed for each double mutant line. We generated the following allelic combinations: *vps29-3 snx1-1*, *vps29-4 snx1-2*, *vps29-5 snx1-1*, *vps29-3 pin1-6*, *vps29-5 pin1-6*, *vps29-3 pid14*, and *vps29-5 pid14*. Within each double mutant line, similar results were found. For introgression of marker lines (*SNX1-GFP*, *GFP-RABF2b*, *GNOM-GFP*, *PIN1-GFP*, *PIN2-GFP*, *AUX1-YFP*, *GFP-LTi6b*, *GFP-PIP2a*, and *DR5-GFP*) in *vps29* mutant background, at least two *vps29* alleles were independently analyzed and gave comparable results.

Microscopy and Drug Treatments

Roots of 7-day-old seedlings grown on MS medium were mounted in LM medium (Jaillais et al., 2006) and analyzed on an LSM-510 Laser-Scanning Confocal Microscope (Zeiss, Jena, Germany). FM4-64, BFA (100 μM in DMSO/EtOH), Wm (33 μM in DMSO), and CHX (50 μm in DMSO) treatments were carried out as described (Jaillais et al., 2006). NAA treatment and analysis of PIN1-GFP lateralization were performed as described (Benkova et al., 2003; Sauer et al., 2006). For *DR5rev:GFP* analysis in cotyledons, a fluorescent stereomicroscope (Leica) coupled with a specific GFP filter set was used. For embryo analysis, siliques were dissected under a stereomicroscope, and

developing seeds were cleared at least 2 hr in chloral hydrate (80 g in 30 ml H_2O and 10 ml glycerol) and observed under a Nikon microscope coupled to a DIC optic. FRAP experiments were performed on an LSM-510 confocal microscope and analyzed with ImageJ software (http://rsb.info.nih.gov/ij/). The pixel intensity of each region of interest (ROI) determined before FRAP was reported as 100% of pixel intensity. After FRAP, the pixel intensity of each ROI corresponded to the percentage of pixel intensity compared with the initial value. Each experiment was repeated at least three times independently and more than ten roots or siliques were analyzed per experiment.

Expression, Localization, and Protein Interaction Analyses

Recombinant plasmid construction and plant transformation are described in Figure S2, yeast two hybrid and coimmunoprecipitation experiments in Figure S7, analysis of *vps29* vascular tissue in Figure S8, in situ hybridization protocol in Figure S9, and immunolocalization in Figure S14.

Statistical Analysis of Results

All the experiments presented in this work were repeated at least three times independently. p values indicated for measurement of primary root length and lateral root density were obtained using a two-sided Student's test assuming unequal variances. All calculations were performed using Microsoft Excel 2003.

Supplemental Data

The Supplemental Data for this article can be found online at http://www.cell.com/cgi/content/full/130/6/1057/DC1/.

ACKNOWLEDGMENTS

We thank the Max Planck Institute and the SALK Institute for providing the insertion mutant lines. We acknowledge G. Jürgens, J. Friml, B. Scheres, M. Bennett, J. Takano, T. Vernoux, K. Schumacher, M. Vidal, R. Tsien, A. Chaboud, and the NASC for providing materials. We thank C. Lionnet and F. Simian for technical assistance in confocal microscopy at PLATIM IFR 128; I. Anselme-Bertrand for technical assistance in scanning electron tomography (SEM) at University Jean Monnet, Saint-Etienne, France; M. Becchi and I. Zanella-Cléon for mass spectrometry analysis at CCMP IFR 128; and T. Vernoux and all members of the SiCE team for fruitful discussions.

Received: April 16, 2007
Revised: June 4, 2007
Accepted: August 27, 2007
Published: September 20, 2007

REFERENCES

Abas, L., Benjamins, R., Malenica, N., Paciorek, T., Wirniewska, J., Moulinier-Anzola, J.C., Sieberer, T., Friml, J., and Luschnig, C. (2006). Intracellular trafficking and proteolysis of the *Arabidopsis* auxin-efflux facilitator PIN2 are involved in root gravitropism. Nat. Cell Biol. *8*, 249–256.

Alonso, J.M., Stepanova, A.N., Leisse, T.J., Kim, C.J., Chen, H., Shinn, P., Stevenson, D.K., Zimmerman, J., Barajas, P., Cheuk, R., et al. (2003). Genome-wide insertional mutagenesis of *Arabidopsis thaliana*. Science *301*, 653–657.

Benkova, E., Michniewicz, M., Sauer, M., Teichmann, T., Seifertova, D., Jurgens, G., and Friml, J. (2003). Local, efflux-dependent auxin gradients as a common module for plant organ formation. Cell *115*, 591–602.

Blilou, I., Xu, J., Wildwater, M., Willemsen, V., Paponov, I., Friml, J., Heidstra, R., Aida, M., Palme, K., and Scheres, B. (2005). The PIN auxin efflux facilitator network controls growth and patterning in *Arabidopsis* roots. Nature *433*, 39–44.

Bonifacino, J.S., and Rojas, R. (2006). Retrograde transport from endosomes to the trans-Golgi network. Nat. Rev. Mol. Cell Biol. *7*, 568–579.

Christensen, S.K., Dagenais, N., Chory, J., and Weigel, D. (2000). Regulation of auxin response by the protein kinase PINOID. Cell *100*, 469–478.

Collins, B.M., Skinner, C.F., Watson, P.J., Seaman, M.N., and Owen, D.J. (2005). Vps29 has a phosphoesterase fold that acts as a protein interaction scaffold for retromer assembly. Nat. Struct. Mol. Biol. *12*, 594–602.

Coudreuse, D., and Korswagen, H.C. (2007). The making of Wnt: new insights into Wnt maturation, sorting and secretion. Development *134*, 3–12.

Coudreuse, D.Y., Roel, G., Betist, M.C., Destree, O., and Korswagen, H.C. (2006). Wnt gradient formation requires retromer function in Wnt-producing cells. Science *312*, 921–924.

Cutler, S.R., Ehrhardt, D.W., Griffitts, J.S., and Somerville, C.R. (2000). Random GFP:cDNA fusions enable visualization of subcellular structures in cells of *Arabidopsis* at a high frequency. Proc. Natl. Acad. Sci. USA *97*, 3718–3723.

Damen, E., Krieger, E., Nielsen, J.E., Eygensteyn, J., and van Leeuwen, J.E. (2006). The human Vps29 retromer component is a metallo-phosphoesterase for a cation-independent mannose 6-phosphate receptor substrate peptide. Biochem. J. *398*, 399–409.

Dettmer, J., Hong-Hermesdorf, A., Stierhof, Y.D., and Schumacher, K. (2006). Vacuolar H+-ATPase activity is required for endocytic and secretory trafficking in *Arabidopsis*. Plant Cell *18*, 715–730.

Friml, J., Vieten, A., Sauer, M., Weijers, D., Schwarz, H., Hamann, T., Offringa, R., and Jurgens, G. (2003). Efflux-dependent auxin gradients establish the apical-basal axis of *Arabidopsis*. Nature *426*, 147–153.

Furutani, M., Vernoux, T., Traas, J., Kato, T., Tasaka, M., and Aida, M. (2004). PIN-FORMED1 and PINOID regulate boundary formation and cotyledon development in *Arabidopsis* embryogenesis. Development *131*, 5021–5030.

Galweiler, L., Guan, C., Muller, A., Wisman, E., Mendgen, K., Yephremov, A., and Palme, K. (1998). Regulation of polar auxin transport by AtPIN1 in *Arabidopsis* vascular tissue. Science *282*, 2226–2230.

Geldner, N., Friml, J., Stierhof, Y.D., Jurgens, G., and Palme, K. (2001). Auxin transport inhibitors block PIN1 cycling and vesicle trafficking. Nature *413*, 425–428.

Geldner, N., Anders, N., Wolters, H., Keicher, J., Kornberger, W., Muller, P., Delbarre, A., Ueda, T., Nakano, A., and Jurgens, G. (2003). The *Arabidopsis* GNOM ARF-GEF mediates endosomal recycling, auxin transport, and auxin-dependent plant growth. Cell *112*, 219–230.

Geldner, N., Richter, S., Vieten, A., Marquardt, S., Torres-Ruiz, R.A., Mayer, U., and Jurgens, G. (2004). Partial loss-of-function alleles reveal a role for GNOM in auxin transport-related, post-embryonic development of *Arabidopsis*. Development *131*, 389–400.

Griffin, C.T., Trejo, J., and Magnuson, T. (2005). Genetic evidence for a mammalian retromer complex containing sorting nexins 1 and 2. Proc. Natl. Acad. Sci. USA *102*, 15173–15177.

Jaillais, Y., Fobis-Loisy, I., Miege, C., Rollin, C., and Gaude, T. (2006). AtSNX1 defines an endosome for auxin-carrier trafficking in *Arabidopsis*. Nature *443*, 106–109.

Lavy, M., Bloch, D., Hazak, O., Gutman, I., Poraty, L., Sorek, N., Sternberg, H., and Yalovsky, S. (2007). A Novel ROP/RAC effector links cell polarity, root-meristem maintenance, and vesicle trafficking. Curr. Biol. *17*, 947–952.

Leyser, O. (2006). Dynamic integration of auxin transport and signalling. Curr. Biol. *16*, R424–R433.

Li, H., Shen, J.J., Zheng, Z.L., Lin, Y., and Yang, Z. (2001). The Rop GTPase switch controls multiple developmental processes in *Arabidopsis*. Plant Physiol. *126*, 670–684.

Oliviusson, P., Heinzerling, O., Hillmer, S., Hinz, G., Tse, Y.C., Jiang, L., and Robinson, D.G. (2006). Plant retromer, localized to the prevacuolar compartment and microvesicles in *Arabidopsis*, may interact with vacuolar sorting receptors. Plant Cell *18*, 1239–1252.

Paciorek, T., Zazimalova, E., Ruthardt, N., Petrasek, J., Stierhof, Y.D., Kleine-Vehn, J., Morris, D.A., Emans, N., Jurgens, G., Geldner, N., and Friml, J. (2005). Auxin inhibits endocytosis and promotes its own efflux from cells. Nature *435*, 1251–1256.

Prasad, B.C., and Clark, S.G. (2006). Wnt signaling establishes anteroposterior neuronal polarity and requires retromer in *C. elegans*. Development *133*, 1757–1766.

Sauer, M., Balla, J., Luschnig, C., Wisniewska, J., Reinohl, V., Friml, J., and Benkova, E. (2006). Canalization of auxin flow by Aux/IAA-ARF-dependent feedback regulation of PIN polarity. Genes Dev. *20*, 2902–2911.

Seaman, M.N. (2005). Recycle your receptors with retromer. Trends Cell Biol. *15*, 68–75.

Shimada, T., Koumoto, Y., Li, L., Yamazaki, M., Kondo, M., Nishimura, M., and Hara-Nishimura, I. (2006). AtVPS29, a Putative Component of a Retromer Complex, is Required for the Efficient Sorting of Seed Storage Proteins. Plant Cell Physiol. *47*, 1187–1194.

Steinmann, T., Geldner, N., Grebe, M., Mangold, S., Jackson, C.L., Paris, S., Galweiler, L., Palme, K., and Jurgens, G. (1999). Coordinated polar localization of auxin efflux carrier PIN1 by GNOM ARF GEF. Science *286*, 316–318.

Swarup, R., Kargul, J., Marchant, A., Zadik, D., Rahman, A., Mills, R., Yemm, A., May, S., Williams, L., Millner, P., et al. (2004). Structure-function analysis of the presumptive *Arabidopsis* auxin permease AUX1. Plant Cell *16*, 3069–3083.

Takano, J., Miwa, K., Yuan, L., von Wiren, N., and Fujiwara, T. (2005). Endocytosis and degradation of BOR1, a boron transporter of *Arabidopsis thaliana*, regulated by boron availability. Proc. Natl. Acad. Sci. USA *102*, 12276–12281.

Tao, L.Z., Cheung, A.Y., and Wu, H.M. (2002). Plant Rac-like GTPases are activated by auxin and mediate auxin-responsive gene expression. Plant Cell *14*, 2745–2760.

Vanoosthuyse, V., Tichtinsky, G., Dumas, C., Gaude, T., and Cock, J.M. (2003). Interaction of calmodulin, a sorting nexin and kinase-associated protein phosphatase with the *Brassica oleracea S* locus receptor kinase. Plant Physiol. *133*, 919–929.

Verges, M., Luton, F., Gruber, C., Tiemann, F., Reinders, L.G., Huang, L., Burlingame, A.L., Haft, C.R., and Mostov, K.E. (2004). The mammalian retromer regulates transcytosis of the polymeric immunoglobulin receptor. Nat. Cell Biol. *6*, 763–769.

Vernoux, T., Kronenberger, J., Grandjean, O., Laufs, P., and Traas, J. (2000). PIN-FORMED 1 regulates cell fate at the periphery of the shoot apical meristem. Development *127*, 5157–5165.

Wang, D., Guo, M., Liang, Z., Fan, J., Zhu, Z., Zang, J., Zhu, Z., Li, X., Teng, M., Niu, L., et al. (2005). Crystal structure of human vacuolar protein sorting protein 29 reveals a phosphodiesterase/nuclease-like fold and two protein-protein interaction sites. J. Biol. Chem. *280*, 22962–22967.

Wisniewska, J., Xu, J., Seifertova, D., Brewer, P.B., Ruzicka, K., Blilou, I., Rouquie, D., Benkova, E., Scheres, B., and Friml, J. (2006). Polar PIN localization directs auxin flow in plants. Science *312*, 883.

Xu, J., and Scheres, B. (2005a). Cell polarity: ROPing the ends together. Curr. Opin. Plant Biol. *8*, 613–618.

Xu, J., and Scheres, B. (2005b). Dissection of *Arabidopsis* ADP-RIBOSYLATION FACTOR 1 function in epidermal cell polarity. Plant Cell *17*, 525–536.